DOI: 10.1017/S1431927605507189
Microsc Microanal 11(Suppl 2), 2005

Microstructural Studies of a Directionally Solidified Nb-27Mo-27Cr-9Al-9Si Alloy

Y.L. Hu*, A.L. Vasiliev*, L.C. Zhang*, M. Aindow* and D.M. Shah‡

*Department of Materials Science and Engineering, Institute of Materials Science, Unit 3136, University of Connecticut, Storrs, CT 06269-3136, USA.
‡ Pratt & Whitney, Materials & Process Engineering, E. Hartford, CT 06108, USA.

A wide variety of different refractory intermetallic compounds have been considered as candidate materials for structural applications at elevated temperatures (above 1000˚C). The common problem with these compounds is that they exhibit extremely low ductility and toughness, particularly at ambient temperature. One approach which has been adopted to overcome this problem is the use of alloy compositions which give a combination of strong refractory intermetallics and ductile toughening phases in the solidification microstructure (e.g. [1-3]). In this paper we describe microstructural data obtained using TEM from one such alloy with a composition Nb-27Mo-27Cr-9Al-9Si (all in atomic %).

The overall microstructure of the alloy consisted of coarse primary dendrites with a fine eutectic mixture in the interdendritic regions (Figs.1&2). Electron diffraction patterns (e.g. Fig. 3) and X-ray spectrometry data (Table 1) obtained from each of the phases revealed that:

- The dendrites are a Mo-rich A2 (BCC) solid solution.
- The eutectic is a lamellar or rod-like mixture of two intermetallic phases: a cubic A15 Nb_3Al-type phase, and a hexagonal C14 Cr_2Nb-type Laves phase. The site occupancies in these phases require further investigation.
- Occasional narrow strips of the cubic C15 Laves phase were also found, but only at the boundary between eutectic A15 and primary A2 phases, suggesting that local constraints may favor the formation of this phase. One example is shown in Fig. 1(b).

Analyses of the diffraction data revealed no simple orientation relationship (OR) between the A2 dendrites and the eutectic colonies. The diffraction data from the A15 and C14 phases within a particular colony indicated that the phases exhibit a relatively simple OR. We note, however, that there is no singular OR for the colonies: at least four crystallographically distinct ORs have been identified thus far. Fig 3 contains examples of the diffraction data from two colonies which exhibit different relationships: OR1 (Figs 3(a)&(b)) and OR2 (Figs 3(c)&(d)). Although the OR varies from colony to colony, facetted interfaces were observed in each case, indicating that there are preferred low-energy interface orientations. Simple geometric analyses of the lattice points in the preferred interfacial facets for several regions have shown that, in each colony, the predominant facet is one in which the interfacial misfit is less than ≈2%. As such, it may be the similarity of various lattice spacings in these two phases that permits the development of colonies with such diverse ORs.

References
[1] D.M. Shah, D.L. Anton, D.P. Pope, S. Chin, Mater Sci Eng, A192/193 (1995) 658.
[2] T. S. Rong, D. N. Horspool, M. Aindow, Intermetallics, 10 (2002) 1.
[3] W-Y Kim, I-D Yoe, M-S Kim and S. Hanada, Mater Trans, 43 (2002) 3254.

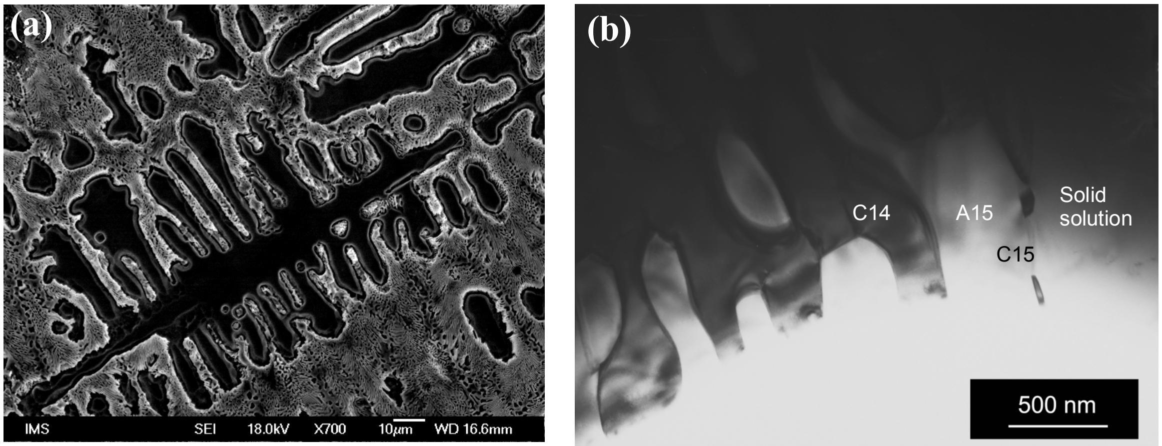

Fig. 1 Overall features of the microstructure (a) secondary electron SEM image (b) bright field TEM image

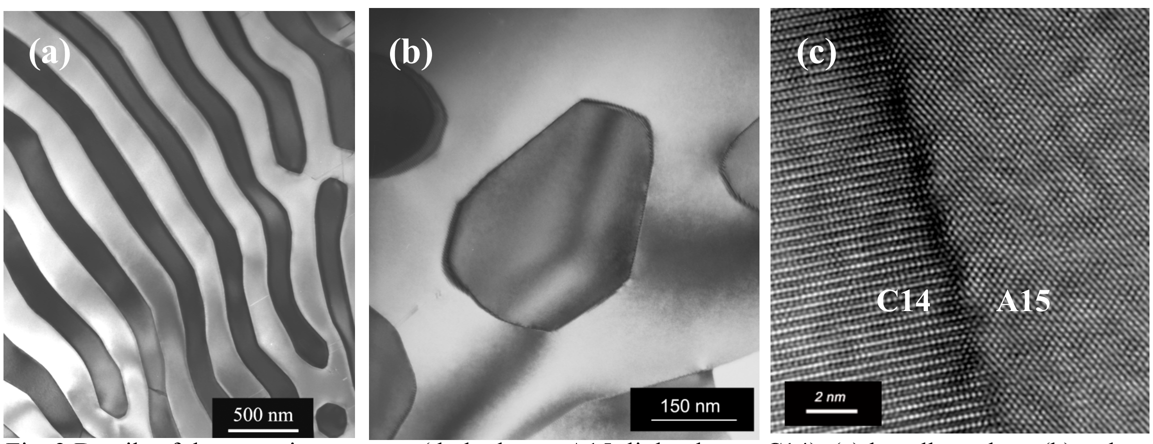

Fig. 2 Details of the eutectic structure: (dark phase - A15, light phase - C14). (a) lamellar colony (b) rod-like colony (C) HRTEM image of an interfacial facet in a rod-like colony.

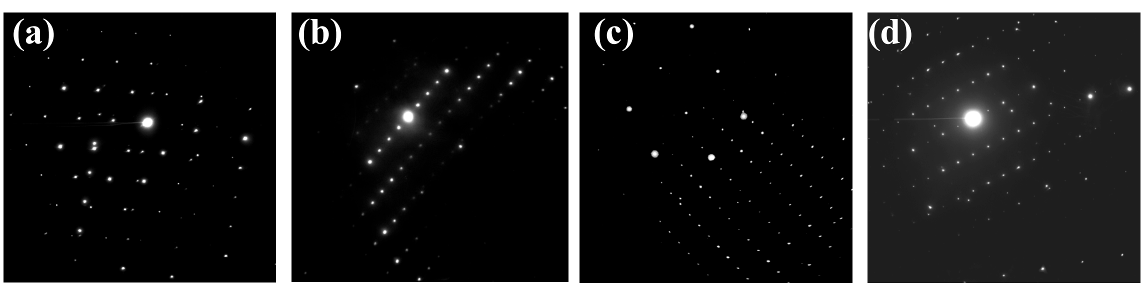

Fig. 3 Diffraction patterns obtained from A15/C14 eutectic colonies. (a) OR1, $B=[1\bar{1}1]_{A15}//[0\bar{1}10]_{C14}$; (b) OR1, $B=[3\bar{5}1]_{A15}//[1\bar{2}10]_{C14}$; (C) OR2, $B=[2\bar{4}\bar{1}]_{A15}//[1\bar{2}10]_{C14}$; (d) OR2, $B=[2\bar{2}3]_{A15}//[2\bar{1}\bar{1}0]_{C14}$.

Table 1: Standard-less energy-dispersive X-ray spectrometry data from the three main phases in the alloy.

Phase	**Composition (atomic %)**				
	Al	**Si**	**Cr**	**Nb**	**Mo**
A15	11.8	8.0	11.8	32.4	35.9
C14	3.9	10.0	34.0	34.0	18.1
A2	7.2	1.7	16.0	33.2	41.9

https://doi.org/10.1017/S1431927605507189 Published online by Cambridge University Press